

Responses of the human visual cortex and LGN to achromatic and chromatic temporal modulations: An fMRI study

Kathy T. Mullen

McGill Vision Research, Department of Ophthalmology,
McGill University, Montreal, Canada



Benjamin Thompson

Department of Optometry and Vision Science,
The University of Auckland, Auckland, New Zealand



Robert F. Hess

McGill Vision Research, Department of Ophthalmology,
McGill University, Montreal, Canada



In this study, we investigate how the responses of the human visual pathway to temporal frequency are modified as information transfers between the lateral geniculate nucleus (LGN) and primary visual cortex (V1) and to the extrastriate areas of the dorsal and ventral streams (V2, V3, VP, V3A, V4, and MT). We use high-field fMRI (4 T) to record simultaneously the responses of these areas across temporal frequency for chromatic stimuli (L/M-cone opponent and S-cone opponent) and stimuli of high and low achromatic contrasts. We find that: (1) the LGN has relatively low-pass responses for temporal frequency at both high and low achromatic contrasts, indicating that LGN cell spiking activity is not well reflected in the BOLD response. In addition, M cell-like temporal responses were not found, even at low contrasts. (2) Responses in V1 and extrastriate areas V2, V3, VP, and V3A display a progressively low-pass dependence on temporal frequency for achromatic stimuli (2–16 Hz) and are flat for chromatic stimuli (2–8 Hz), showing little overall difference between chromatic and achromatic cortical temporal filtering. (3) Strongly differential effects are found between dorsal and ventral stream processing by the level of MT and V4. V4 shows a significant low-pass temporal dependence for all achromatic and chromatic stimuli, whereas MT has temporally high-pass or flat responses for achromatic and chromatic stimuli. MT was the only visual area that showed M cell-like responses. We conclude that the dorsal and ventral pathways of human vision progressively develop characteristic differences in temporal processing that affect both chromatic and achromatic stimuli.

Keywords: LGN, visual cortex, color, temporal frequency, S-cone, L/M-cone opponent, fMRI, V1, V4, MT

Citation: Mullen, K. T., Thompson, B., & Hess, R. F. (2010). Responses of the human visual cortex and LGN to achromatic and chromatic temporal modulations: An fMRI study. *Journal of Vision*, 10(13):13, 1–19, <http://www.journalofvision.org/content/10/13/13>, doi:10.1167/10.13.13.

Introduction

Temporal frequency is a fundamental parameter in determining visual sensitivity and has been investigated extensively at both the psychophysical and single cell level. Psychophysically, temporal frequency reveals important distinctions between the chromatic and achromatic pathways; color contrast sensitivity is temporally low-pass, declining after 1–2 Hz and with a low temporal resolution of approximately 16 Hz (Kelly, 1983), whereas achromatic contrast sensitivity is band-pass, peaking around 10 Hz with a high-resolution cut-off near 60 Hz (Robson, 1966). There is evidence from primate neurophysiology that these differences in temporal characteristics begin to emerge at the level of the retina and lateral geniculate nucleus (LGN). The chromatic response, carried by sustained parvocellular cells, operates over a relatively lower temporal range than the achromatic

response of either parvocellular (P) or magnocellular (M) cells in the LGN (Derrington & Lennie, 1984; Lankheet, Lennie, & Krauskopf, 1998; Reid & Shapley, 2002). It is important to note, however, that both of these LGN cell types respond to temporal frequencies that are considerably higher than can be detected psychophysically, indicating that further temporal filtering operates at a subsequent cortical stage. In fact, primate cortical neurons in V1 respond over a lower temporal range than the subcortical structures (Foster, Gaska, Nagler, & Pollen, 1985), and further extrastriate cortical filtering is likely to occur specific to the specialized functions of dorsal and ventral cortical pathways. Little is known about how the response to temporal frequency changes in color responsive cells in the cortex.

In this paper, we use fMRI to investigate the response properties of the LGN and six different visual areas of the human cortex to temporal frequency in both the achromatic and chromatic domains. A recent fMRI investigation has shown that robust chromatic responses of the human LGN

can be recorded at 2 Hz (Mullen, Dumoulin, & Hess, 2008). It is also established that the visual areas of the ventral cortical stream have strong responses to color that match or exceed those to achromatic contrast (Brewer, Liu, Wade, & Wandell, 2005; Engel, Zhang, & Wandell, 1997; Hadjikhani, Liu, Dale, Cavanagh, & Tootel, 1998; Kleinschmidt, Lee, Requardt, & Frahm, 1996; Liu & Wandell, 2005; McKeefry & Zeki, 1997; Mullen, Dumoulin, McMahon, De Zubicaray, & Hess, 2007; Mullen, Thompson, & Hess, 2008; Wade, Augath, Logothetis, & Wandell, 2008; Wade, 2002; Wade, Brewer, Rieger, & Wandell, 2002; Wandell, Brewer, & Dougherty, 2005). Here we investigate the responses to achromatic stimuli and two types of chromatic stimuli (the S-cone opponent and L/M-cone opponent) as a function of temporal frequency. This is done for the visual areas in the ventral pathway, which is specialized for color, and for the dorsal pathway, which is strongly dependent on the achromatic M cell visual input (Maunsell, Nealey, & DePriest, 1990).

The achromatic response across temporal frequency has been investigated in several previous fMRI studies, although these have produced conflicting results. Singh, Smith, and Greenlee (2000) reported similar band-pass functions for all retinotopic cortical areas, including MT, with a peak around 9 Hz; they point out that this corresponds to the peak of the human temporal contrast sensitivity function for the spatial frequency used (2 cycles/degree). No measurements were made of the LGN response. Kastner et al. (2004), on the other hand, found high-pass responses in all the cortical areas tested, with responses rising as a function of flicker rate up to the highest temporal frequency used (10 Hz, although called 20 Hz due to a definition of temporal frequency as two times higher than that normally used, see *Discussion* section). Kastner et al. (2004) included the LGN in their measurements, which also showed a high-pass dependence on temporal frequency. Thus, there is a considerable discrepancy between reported responses to achromatic flicker for reasons that are unclear, but may include the different spatial properties of the stimuli, the way temporal frequency is defined, and the different temporal waveforms of the flicker used.

In color vision, there are no systematic fMRI studies on the effects of temporal frequency on BOLD responses, although some studies have included temporal frequencies as a parameter in cortical fMRI investigations (Engel et al., 1997; Jiang, Zhou, & He, 2007; Liu & Wandell, 2005; Wade et al., 2008). Two of these studies reported differential effects of two temporal frequencies that depended on the visual cortical area tested and whether achromatic or chromatic contrast was used (Liu & Wandell, 2005; Wade et al., 2008). Here we explore these differential effects systematically across temporal frequency and visual area with chromatic and achromatic contrasts, including the LGN and a range of cortical areas. Important features of our design are that we use narrowband spatiotemporal sinusoidal stimuli modulated in three different directions

in color space to isolate the L/M-cone opponent, S-cone opponent, and achromatic pathways, respectively. We also use a design that allows the presentation of three sinusoidal temporal frequencies within one scan allowing direct comparison across temporal frequency under each chromatic or achromatic condition. For the achromatic condition, both high and low contrasts were used as M and P cell pathways are differentially sensitive to contrast level, with M cells, but not P cells, responding well at low contrasts (below 10%; Kaplan & Shapley, 1982; Lee, Pokorny, Smith, Martin, & Valberg, 1990; Sclar, Maunsell, & Lennie, 1990; Shapley, 1982). We compare these achromatic and chromatic responses in the human LGN and in six retinotopically mapped visual cortical areas (V1, V2, V3, VP, V4, and human MT), thus spanning both the ventral and dorsal visual pathways.

Materials and methods

Subjects

Six healthy observers were used as subjects (4 females, 2 males), four of whom were naive to the purpose of the study. Of these, five were used in the cortical analyses. All observers had normal, or corrected-to-normal, visual acuity. No participant had a history of psychiatric or neurological disorder, head trauma, or substance abuse. Informed written consent was gained from all participants prior to the commencement of the study. The study was conducted within the constraints of the ethical clearance from the Medical Research Ethics Committee of the University of Queensland for MRI experiments on humans at the Centre for Magnetic Resonance and conforms to the Code of Ethics of the World Medical Association (Declaration of Helsinki).

Visual stimuli

The stimuli were radial sinewave gratings (0.5 cycle/degree) whose contrast sinusoidally phase reversed at 2 Hz, 8 Hz, or 16 Hz for achromatic stimuli and at 2 Hz, 4 Hz, or 8 Hz for the two chromatic stimuli (see Mullen, Dumoulin et al., 2008; Mullen et al., 2007 for pictures of the ring stimuli). The highest temporal frequency of 16 Hz was not used in the experiments with chromatic stimuli, as these stimuli appeared faint and achromatic (see later discussion). Although it has been shown that V1 may respond to undetectable chromatic flicker (Jiang et al., 2007), we required subjects to be able to attend to all stimuli equally. All stimuli were presented in a temporal Gaussian contrast envelope ($\sigma = 125$ ms).

Three different stimulus types were used that isolate the L/M-cone opponent, S-cone opponent, and achromatic

(luminance) post-receptoral mechanisms, termed, respectively, red-green (RG), blue–yellow (BY), and achromatic (Ach).¹ The cone contrasts of the chromatic stimuli were set high relative to threshold, creating highly visible stimuli and maximizing signal strength: 44% for the S-cone condition, 4.0% for the L/M-cone condition, and 54% for the achromatic condition, corresponding to approximately 37, 25, and 24 times threshold for the BY, RG, and Ach stimuli, respectively, presented at 2 Hz. In addition, a low-contrast condition (8%) was run for the achromatic stimuli. The stimuli were viewed as 16 degrees (full width) by approximately 12 degrees (full height), since stimulus height was limited top and bottom by the subject's placement in the magnet bore. A small fixation dot was present in the center of the stimulus. This radial arrangement permitted a spatially narrowband stimulus to be displayed at a relatively low spatial frequency. A spatial frequency of 0.5 cycle/degree was chosen to avoid artifacts generated by chromatic aberration in the chromatic stimuli (Bradley, Zang, & Thibos, 1992; Cottaris, 2003) and to optimize chromatic contrast sensitivity (Mullen, 1985). Spatial frequency was not varied experimentally due to these constraints.

Chromatic representation

The stimulus chromaticity was defined using a 3-dimensional cone contrast space in which each axis represents the quantal catch of the L-, M-, and S-cone types normalized with respect to the white background (i.e., cone contrast). Stimulus chromaticity is given by the vector direction and contrast by vector length within the cone contrast space. Three cardinal stimuli (RG, BY, and Ach) were determined within this space isolating each of the three different post-receptoral mechanisms. A cardinal stimulus isolates one post-receptoral mechanism and is invisible to the other two and, hence, is defined as the direction in cone contrast space orthogonal to the vector directions representing the other two post-receptoral mechanisms (Cole, Hine, & McIlhagga, 1993). We selected our three cardinal stimuli from a knowledge of the cone weights of the three post-receptoral mechanisms provided by earlier studies (Cole et al., 1993; Sankeralli & Mullen, 1996, 1997), and they have the following directions in the cone contrast space: the achromatic (Ach) stimulus activates L-, M-, and S-cones equally (weights of 1, 1, and 1, respectively), the blue–yellow (BY) stimulus activates S-cones only (weights of 0, 0, and 1), and the isoluminant red–green (RG) stimulus activates L- and M-cones oppositely in a proportion determined by the isoluminant point and has no S-cone activation (weights of 1, $-a$, and 0). The ratio of L- to M-cone weights for red–green isoluminance (value of a above) was based on an average determined previously using a minimum motion method (Mullen et al., 2007).

Apparatus and calibrations

For all the fMRI experiments, visual stimuli were generated using PsychToolbox software (Brainard, 1997; Pelli, 1997) on a Macintosh G3 iBook and displayed on a white screen using an LCD projector (InFocus LP250, resolution of 1024×768 , frame rate = 80 Hz, mean luminance = 30 cd/m^2). The screen was placed 2.7 m from the subject. For the psychophysical experiments used to determine detection threshold and isoluminance, stimuli were generated using a VSG 2/5 graphics board with 15 bits of contrast resolution (Cambridge Research Systems, Rochester, England) housed in a Pentium PC computer and displayed on a CRT monitor (Diamond Pro 2030). We estimated any contrast loss of the stimuli presented on the LCD display occurring as a function of temporal frequency by using the formulas of Zhang, Teunissen, Song, and Li (2008), which describe the (dynamic) modulation transfer functions of LCDs at different stimulus speeds. Our highest temporal frequency of 16 Hz has a maximum contrast attenuation of 3.5%, which we considered too small to correct, with no contrast loss for 2–8 Hz. These attenuations are similar to those reported by Liu and Wandell (2005). Both projection and CRT displays were linearized and color calibrated in the same way. The red, green, and blue spectral emissions were measured using a PhotoResearch PR-650-PC SpectraScan (Chatsworth, CA), and the Smith and Pokorny fundamentals (Smith & Pokorny, 1975) were used for the spectral absorptions of the L-, M-, and S-cones. From these data, a linear transform was calculated to specify the phosphor contrasts required for given cone contrasts (Cole & Hine, 1992). Both displays were gamma corrected in software with lookup tables. The cone contrast gamut is most limited in the red–green direction, with an upper cone contrast limit for the projection system of 5.5% for the RG stimuli, depending precisely on the calibration data and the projector settings.

Experimental protocols and stimulus contrasts

Four different stimulus conditions were presented in a block design in each scan: the three different temporal frequencies and a mean luminance (blank) condition in which only the fixation stimulus appeared, all presented at the same color and cone contrast. The fixation condition was a ring of the same chromaticity as the stimulus surrounding a small fixation spot (modulated at 2 Hz). Stimuli were presented time-locked to the acquisition of fMRI time frames, i.e., every 3 s. To control for attention, which can modulate activity in both LGN (O'Connor, Fukui, Pinsk, & Kastner, 2002) and cortex (Brefczynski & DeYoe, 1999; Gandhi, Heeger, & Boynton, 1999; Somers, Dale, Seiffert, & Tootel, 1999), subjects continuously performed a two-interval forced-choice (2AFC) contrast

discrimination task, in which a given presentation consisted of two intervals, both displaying stimuli from the same condition but with a small near-threshold contrast difference between them. Subjects were instructed to maintain fixation on the fixation point and were trained prior to the scanning sessions to familiarize themselves with the task. The subject indicated which interval contained the higher contrast stimulus. The contrast difference between the 2AFC presentations ranged between $\pm 10\%$ and $\pm 20\%$ of the mean contrast for each stimulus type and was selected based on psychophysical measurements on three subjects prior to scanning. The same contrast increments were given to all subjects. This method yielded an overall average discrimination of 92% correct, with consistent performances across color condition and temporal frequency indicating that attention was well controlled (Mullen et al., 2007).

Each stimulus was presented within a 500-ms time window in its temporal Gaussian contrast envelope ($\sigma = 125$ ms), with an inter-stimulus interval of 500 ms. In the remaining 1.5 s, the subjects' responses were recorded using an MR compatible computer mouse. During the fixation (blank) condition, an identical contrast discrimination task was performed for the fixation stimulus. The three temporal frequencies were presented in a counterbalanced block design. Six presentations of one of the temporal frequencies (duration = 18 s) were followed by three presentations of the fixation condition (9 s), repeated for each temporal frequency in quasi-random order. Each block was repeated 9 times with 3 blank presentations at scan onset, giving a total of 273 presentations per scan, i.e., 12 min per scan. All results are based on data from 2 scans per experiment (546 presentations, 24 min).

Magnetic resonance imaging

The magnetic resonance images were acquired using a 4-T Bruker MedSpec system at the Centre for Magnetic Resonance, Brisbane, Australia. A transverse electromagnetic (TEM) head coil was used for radio-frequency transmission and reception (Vaughan et al., 2002). For the functional MRI studies, 241 T2*-weighted gradient-echo echoplanar images (EPI) depicting blood oxygen level-dependent (BOLD) contrasts (Ogawa, Lee, Kay, & Tank, 1990) were acquired in each of the 36 planes with TE = 30 ms, TR = 3000 ms, in-plane resolution = 3.6 mm, and slice thickness = 3 mm (0.6 mm gap). The slices were taken parallel to the calcarine sulcus and covered the entire occipital and parietal lobes and large dorsal-posterior parts of the temporal and frontal lobes. Two to three fMRI scans were performed in each session. Head movement was limited by foam padding within the head coil. In the same session, a high-resolution 3D T1 image was acquired using an MP-RAGE sequence with TI = 1500 ms, TR = 2500 ms, TE = 3.83 ms, and a spatial resolution of 0.9 mm³. Identification of the early visual

cortical areas, including V1, was performed in separate sessions with identical parameters except for the number of time frames (128), number of fMRI scans (1–4), and slice orientation (orthogonal to the calcarine for the retinotopic mapping scans).

Preprocessing of MR images

Data analysis was conducted with the commercially available Brain Voyager analysis package version 1.9.10 (Brain Innovations, Maastricht, The Netherlands). The initial time frame of each functional run was discarded due to start-up magnetization transients in the data. Functional scans were high-pass filtered and motion corrected using subroutines within Brain Voyager. They were then aligned to each subject's high-resolution anatomical images (resampled at 1 mm³) and transformed to Talairach space (Talairach & Tournoux, 1988).

Identification of cortical visual areas and LGN

The retinotopic mapping data were analyzed using volumetric phase-encoded retinotopic mapping (Dumoulin et al., 2003) as previously described (Mullen et al., 2007). By combining eccentricity and polar-angle phase maps (Engel et al., 1994) with the anatomical MRI, the visual field signs could be segmented. V1 was identified as a large mirror-image representation of the visual field in and around the calcarine sulcus.

We identified LGN locations based upon anatomy and two kinds of functional localizers. In both cases, the LGN was defined as a stimulus responsive region in the appropriate anatomical location (Kastner et al., 2004). The first functional localization was conducted in a separate session using a high-contrast flickering (16 Hz) checkerboard stimulus, with chromatic and achromatic contrasts and both AC and DC modulations, compared to a blank, black (dim) screen with a small black fixation dot, as described previously (Hess, Thompson, Gole, & Mullen, 2009; Mullen, Dumoulin et al., 2008). The second localizer was based upon a statistical comparison of all experimental stimuli versus fixation. For both methods, regions of interest (ROIs) were created by first identifying the peak voxel within the LGN anatomical region, then centering a cube of 1000 mm³ (10 × 10 × 10 mm) on the peak voxel, since previous estimates of LGN size fall within this volume (Schneider, Richter, & Kastner, 2004). The ROI was defined as all voxels within the cube, contiguous with the peak voxel, whose activity in response to the stimuli was above threshold at the FDR-corrected level of $q < 0.001$ (Benjamini & Hochberg, 1995). LGN localizations using ring and checkerboard stimuli are similar and slight variations in the position and size of the LGN may be attributed to noise, registration errors, or differences in stimulus layout and content. We chose to define the LGN

ROI based upon the experimental stimuli because that definition minimizes the effect of registration errors and stimulus differences when analyzing the experimental stimuli. Note that this definition of the ROI compares all stimuli versus fixation and therefore does not affect comparisons between different stimuli. Figure 1 shows the LGN ROIs (black dotted outlines) of two of our subjects in coronal section. The Talairach coordinates and size of the LGN ROIs for all subjects are given in Table 1. A statistical comparison shows that our coordinates and volumes are similar to the averages previously reported (Hess et al., 2009; Kastner et al., 2004; Mullen, Dumoulin et al., 2008; O'Connor et al., 2002; Schneider et al., 2004).

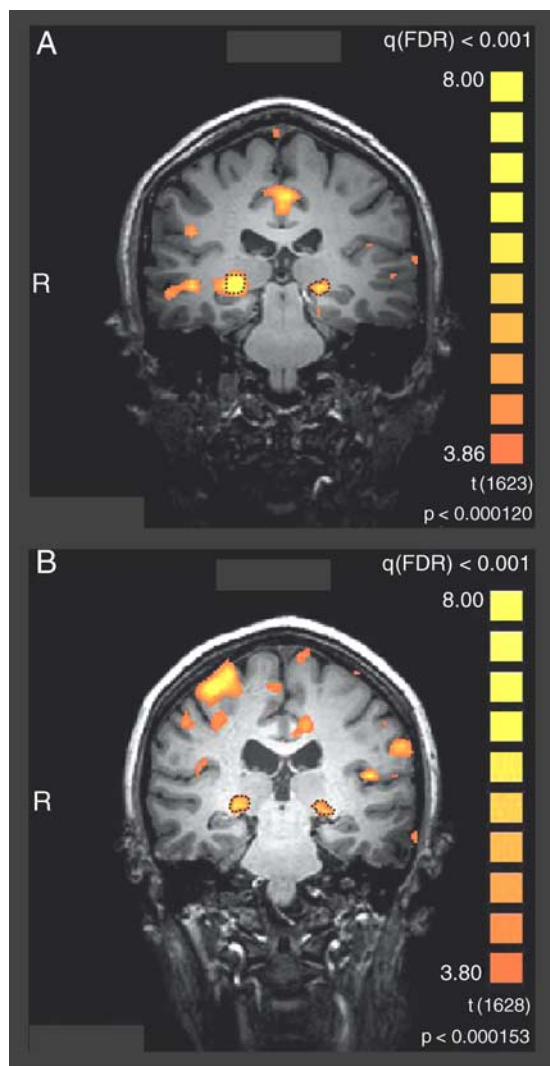


Figure 1. *T*-statistical maps of two subjects ((A) GDZ; (B) JAS) showing coronal views of the left and right hemispheres in stereotaxic space (Talairach & Tournoux, 1988) illustrating typical LGN activations and the defined ROIs, outlined by the black dashed lines for each subject (for coordinates, see Table 1; for ROI definition, see Materials and methods section). *T*-values indicate responses to all stimuli (Ach, RG, and BY) minus the blank (fixation) condition. R indicates right hemisphere.

fMRI and statistical analyses

A general linear model (GLM) analysis using % change time course normalization was conducted on the time courses of voxels within each region of interest (ROI) for each individual participant. This analysis provided beta values for each temporal frequency for each condition. Each beta value represented the variation in the voxel time courses within a specific ROI that could be accounted for by neural activity in response to each temporal frequency and can be expressed as % BOLD signal change. The reference model for the GLM analysis was a standard double gamma hemodynamic response function, with a time to peak of 5 s and a time to undershoot peak of 15 s. For each condition (Ach, BY, and RG), the two scanning runs were analyzed in combination using a multi-study general linear model in order to generate one beta value per temporal frequency.

Beta values were analyzed separately for each condition (Ach-high, Ach-low, RG, and BY). A within-subjects ANOVA (degrees of freedom corrected for sphericity using the Huynh–Feldt correction) with a factor of temporal frequency (2 Hz vs. 8 Hz vs. 16 Hz for the Ach stimuli and 2 Hz vs. 4 Hz vs. 8 Hz for both chromatic stimuli) was used to test for any main effects of temporal frequency within each data set. Since we anticipated that some data sets would show non-monotonic band-pass effects that could not be revealed with an AVOVA, planned paired *t*-tests were also conducted to test for differences between pairs of temporal frequencies. If the ANOVA revealed a main effect of temporal frequency, a critical *p*-value of 0.05 was accepted for the paired *t*-tests. If the main effect was not significant, a Bonferroni corrected critical *p*-value of 0.017 was required for the paired *t*-tests. Responses to temporal frequency were compared across different visual areas or conditions (Ach-low, Ach-high, RG, and BY) using post-hoc ANOVAs.

Separate analyses were conducted for the LGN, V1, V4, and MT as strong temporal frequency and chromaticity effects were anticipated (and observed) in the data. Additional motivations for analyzing V4 and MT separately were the fact that they represent the ventral and dorsal visual processing pathways, respectively, and that they showed effects that were distinct from other visual areas. For the extrastriate visual areas V2, V3, VP, and V3A, a combined analysis was employed for each chromaticity condition using the same AVOVA model with the additional factor of visual area.

Results

LGN response to temporal frequency

Results for the LGN are shown for high-contrast achromatic stimuli (Figure 2A), low-contrast achromatic

Participant	Left			Volume (mm ³)	Right			Volume (mm ³)		
	Talairach coordinates				Talairach coordinates					
	x	y	z		x	y	z			
GDZ	-19	-26	-3.5	466	23	-28	-1.3	764		
JAS	-20	-25	-2.9	385	20	-25	0.1	535		
JDH	-23	-24	-3.8	107	-	-	-	-		
KLM	-21	-24	-4.5	993	17	-29	-1.5	974		
KTM	-20	-26	-1.4	158	24	-22	-2.5	54		
RFH	-26	-25	-4.4	792	23	-27	-4.8	712		
Mean	-21.5	-25	-3.4	484	21.4	-26.2	-2	608		
SD	2.6	0.9	1.2	350	2.9	2.8	1.8	347		

Table 1. The LGN coordinates (mm) and volumes (mm³) located in stereotaxic space (Talairach & Tournoux, 1988) for the six subjects. For one subject, only the left LGN could be localized using our threshold criteria ($q(\text{FDR}) < 0.001$).

stimuli (Figure 2B), L/M-cone opponent stimuli (Figure 2C), and S-cone isolating stimuli (Figure 2D). Time series data for the LGN, corresponding to the histograms in Figure 2, are shown in Figure 3 and demonstrate robust and significant responses to all conditions. Both achromatic contrasts (Figures 2A and 2B) reveal a significantly diminished BOLD response at high temporal frequencies (16 Hz). Responses to the high-contrast achromatic stimuli have a band-pass appearance with a significant loss in BOLD signal occurring between 8 and 16 Hz ($t(5) = 3.6$, $p = 0.016$) but no significant difference between 2 and 8 Hz ($p > 0.017$). For low-contrast achromatic stimuli (Figure 2B), the data clearly show a low-pass shape with a significant loss of response between 2 and 16 Hz ($t(4) = 9.8$, $p < 0.001$). Although a post-hoc ANOVA does not show a significant interaction between contrast level and temporal frequency in these two data sets ($p < 0.05$), likely due to the number of subjects, the different pattern of temporal frequency responses we observe for the low- and high-contrast results may reflect differential contrast gains of the BOLD signal of the LGN with temporal frequency. For example, the results are compatible with a relatively higher contrast gain at the higher temporal frequencies (8 and 16 Hz) compared to the low (2 Hz), a potential effect that requires further investigation.

Low-contrast stimuli are known to favor responses in the M cell pathway (Kaplan & Shapley, 1982; Sclar et al., 1990; Shapley, 1982), with single neurons showing an increasing response with temporal frequency over this temporal range (Derrington & Lennie, 1984; Levitt, Schumer, Sherman, Spear, & Movshon, 2001). Yet, we find that BOLD responses to low-contrast sinusoidal stimuli have a low-pass dependence on temporal frequency with significant loss of response with increasing temporal frequency. Hence, BOLD responses do not show a correspondence to the single cell responses of LGN M cells.

Results for the two chromatic stimuli are shown in the two lower panels (Figure 2C, L/M-cone opponent and Figure 2D, S-cone isolating). For the L/M-cone opponent

(RG) stimuli, the BOLD responses are not significantly different over the temporal frequency range of 2–8 Hz, although there is a slight downward trend with temporal frequency. Likewise for the S-cone isolating stimuli, no significant effect of temporal frequency was found, although there is a slight upward trend. Thus, overall the chromatic responses of the LGN are relatively flat with temporal frequency over the range at which stimuli are visible and chromatic in appearance.

Cortical response to temporal frequency

The cortical results for high- and low-contrast achromatic stimuli are shown in Figure 4 for all visual areas measured, and the equivalent data for the chromatic stimuli are shown in Figure 5. Time series data for the key areas of V1, V4, and MT are shown in Figures 6, 7, and 8, respectively, and demonstrate robust cortical responses across all conditions. Additionally, in Figure 9 we make specific comparisons between results for areas V4 and MT, chosen as visual areas representative of the ventral and dorsal visual streams, respectively. For achromatic stimuli (Figure 4), all V1 results show an overall low-pass shape with temporal frequency. At high achromatic contrasts, there is a reduced response with increasing temporal frequency although this main effect does not reach significance ($p = 0.09$). Planned pairwise comparisons reveal a marginal but non-significant loss of BOLD response between 2 and 8 Hz ($t(4) = 3.6$, $p = 0.022$; $p > 0.017$). At low achromatic contrasts in V1, there was a significant main effect of temporal frequency ($F(2, 6) = 11.24$, $p = 0.009$), with a significant loss in response between the low (2 Hz) and high (16 Hz) temporal frequencies ($t(3) = 5.4$, $p = 0.012$).

The analyses of the extrastriate areas V2, V3, VP, and V3A were combined into one ANOVA (see fMRI and statistical analyses section of Materials and methods section). Both the high- and low-contrast achromatic conditions

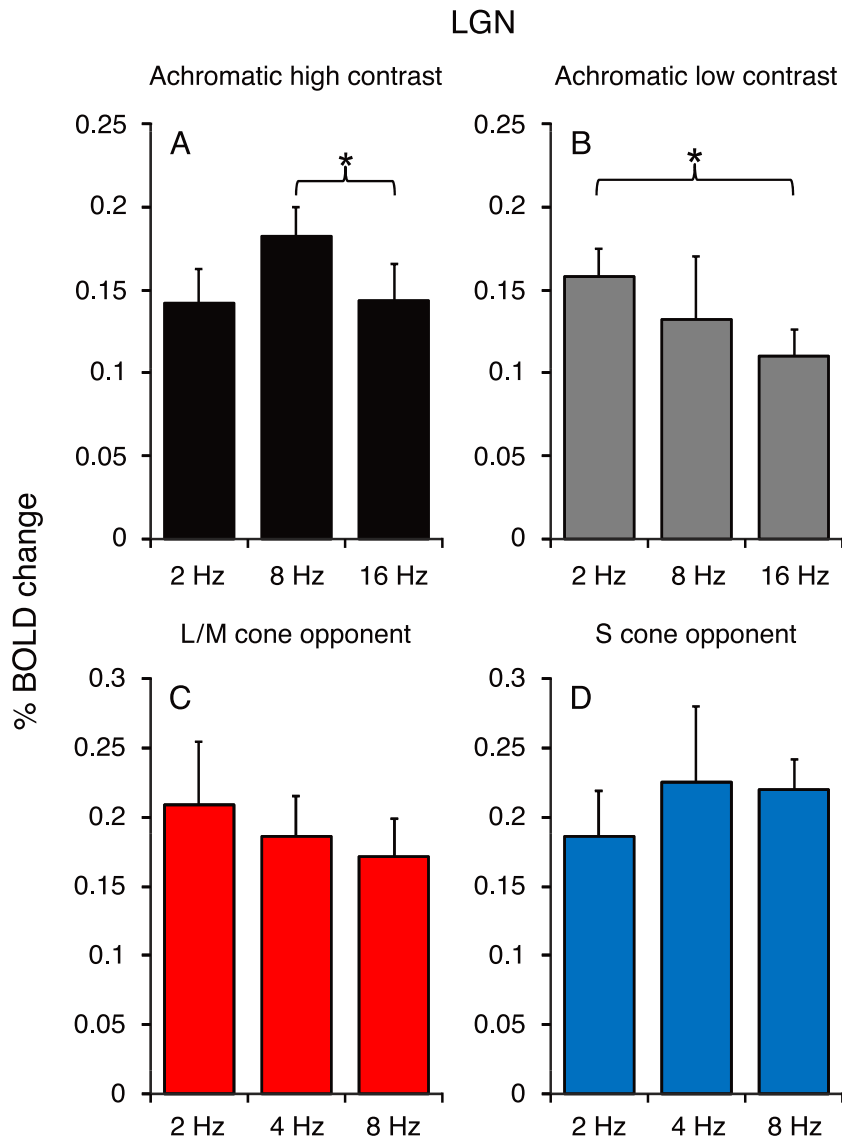


Figure 2. Results for the LGN. Percent BOLD signal is plotted as a function of temporal frequency for stimulus types with contrasts in parentheses as follows: (A) achromatic high contrast (54%), (B) achromatic low contrast (8%), (C) L/M-cone opponent (4%), (D) S-cone opponent (44%). Note the different temporal frequency ranges for the achromatic and chromatic stimuli; * indicates significant pairwise differences ($p < 0.017$). The plots show the average and $+1$ standard error of the mean of 6 subjects, except for the low-contrast Ach condition for which 5 subjects were used.

show a significant main effect of temporal frequency (high contrast: $F(3, 12) = 20.1, p = 0.001$; low contrast: $F(3, 9) = 10.4, p = 0.011$) confirming the low-pass shape that is clearly visible in the data. In addition, the response in all of these areas, for both the low- and high-contrast conditions, is significantly lower for the 16-Hz stimuli than for the 2-Hz stimuli ($p < 0.05$). For the high-contrast condition, there is also a reliable difference between the 2-Hz and 8-Hz stimuli for all areas ($p < 0.05$). These results clearly demonstrate the low-pass temporal characteristics of these extrastriate areas at both high and low-contrast levels.

Area V4 (Figures 4 and 9) displays the same low-pass dependence on temporal frequency as the other extrastriate areas analyzed above. Both the high- and low-contrast

achromatic conditions show a significant main effect of temporal frequency (high contrast: $F(2, 8) = 22.5, p = 0.001$; low contrast: $F(2, 6) = 13.5, p = 0.006$). In addition, in both high and low achromatic contrast conditions, the BOLD responses to the mid- and high temporal frequencies (8 and 16 Hz) fall significantly below the low temporal frequency (2 Hz; high contrast, 8 vs. 2 Hz: $t(4) = 4.1, p = 0.015$; low contrast, 8 vs. 2 Hz: $t(3) = 4.4, p = 0.02$; high contrast, 16 vs. 2 Hz: $t(4) = 7.0, p = 0.002$; low contrast, 16 vs. 2 Hz: $t(3) = 4.7, p = 0.019$).

Area MT (Figures 4 and 9), on the other hand, shows a significantly different pattern of results from those of V4 for both achromatic stimuli (see legend of Figure 9). For the high-contrast condition, the dependence on temporal

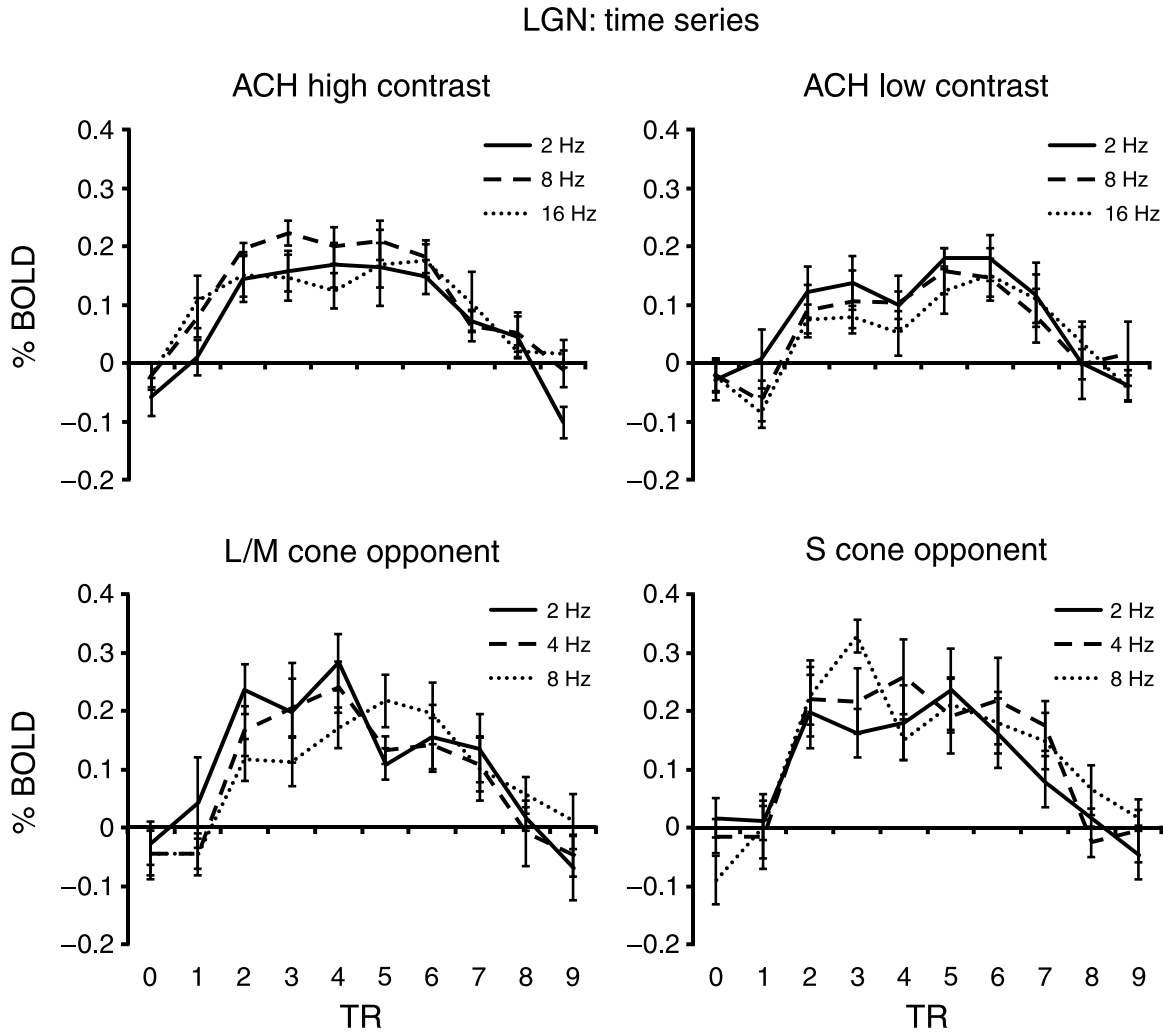


Figure 3. Time series data for the LGN showing each temporal frequency (solid, dashed, and dotted lines) and each color condition (Ach high contrast, Ach low contrast, L/M-cone opponent, and S-cone opponent) as marked. Stimulus onset was at TR = 0 and offset at TR = 6 (i.e., stimuli were presented in 6 TRs). TR (repetition time) = 3 s. Data are the responses (% BOLD) normalized to the preceding two blank (fixation) presentations and are averaged across subjects. Error bars show the between-subjects standard error of the mean.

frequency is high pass with a significant main effect of temporal frequency ($F(2, 6) = 14.4, p = 0.002$) that runs in the opposite direction from all other areas, as responses to both mid- (8 Hz; $t(4) = 8.8, p \leq 0.001$) and high (16 Hz; $t(4) = 4.3, p = 0.013$) temporal frequencies are significantly greater than to the low frequency (2 Hz). For the low-contrast condition, the high-pass shape is not apparent, with the results appearing flat with no significant effects across temporal frequency ($p > 0.05$). The differences between the two achromatic contrasts are significant (see legend of Figure 9) and suggest a variation in contrast gain with temporal frequency. The time series data of MT (Figure 8) indicate that the responses at the low temporal frequency (2 Hz) saturate at low contrasts, but the responses at 16 Hz increase with contrast.

The results for the chromatic stimuli are shown in Figures 5 and 9 for the L/M- and S-cone opponent conditions, respectively. For V1 (Figure 5), there is no effect of temporal frequency (2–8 Hz) on either the L/M-

cone opponent or the S-cone opponent chromatic responses. Similarly, for the extrastriate areas (V2, V3, VP, and V3A), we found no effect of temporal frequency for either chromatic condition. Although there is a visible trend for low-pass responses for the S-cone isolating stimuli, this main effect did not reach significance ($p = 0.08$). Only one area, VP, revealed a reliable difference between temporal frequencies for BY stimuli (after correction for multiple comparisons), whereby there was a significant loss of BOLD response at the high (8 Hz) temporal frequency ($t(4) = 4.0, p = 0.016$).

The chromatic data for area V4 (Figures 5 and 9) reveal a significant dependence on temporal frequency with low-pass effects for both L/M-cone opponent and S-cone opponent stimuli (L/M-cone: $F(2, 9) = 7.0, p = 0.017$; S-cone: $F(2, 10) = 6.4, p = 0.022$). The pattern of responses across temporal frequency is significantly different from those seen in V1 for both chromatic conditions (RG, $F(1, 2) = 12.3, p = 0.017$; BY, $F(1, 2) = 4.7, p =$

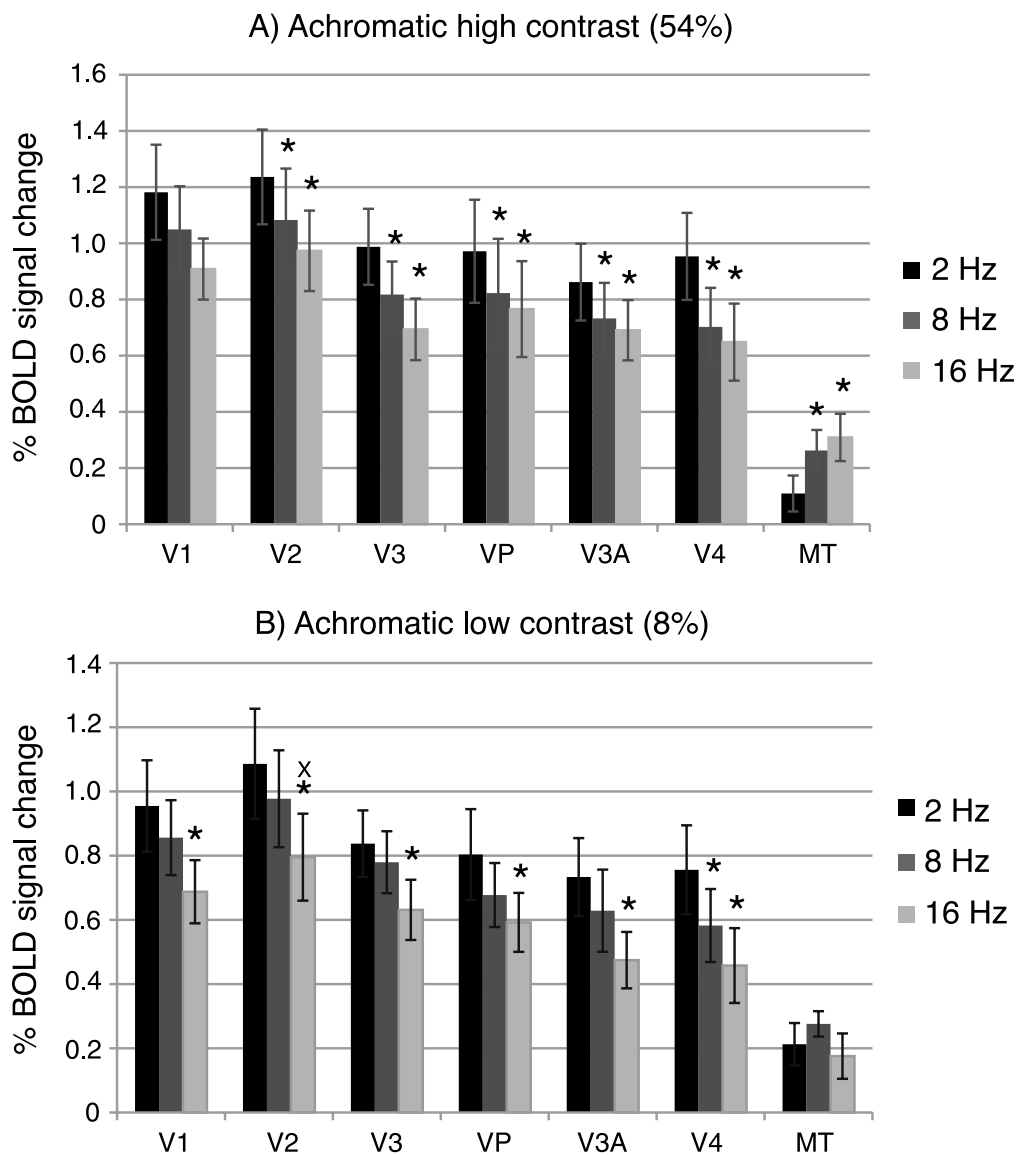


Figure 4. Results for achromatic stimuli in cortical areas V1, V2, V3, VP, V3A, V4, and MT. Percent BOLD signal is plotted as a function of 3 temporal frequencies (TF; 2, 8, and 16 Hz) in each cortical area for (A) high- and (B) low-contrast achromatic stimuli. Histograms show the means ± 1 SE for five (A) or four (B) subjects. Data were analyzed using ANOVAs (see Statistical analyses and Results sections). A general low-pass response can be seen in all cortical areas with the exception of MT, which shows a high-pass response to the high-contrast stimulus and a flat response to the low-contrast stimulus. All areas: “**” indicates a significant ($p \leq 0.05$) difference from 2 Hz; “ \times ” indicates a significant difference from 8 Hz.

0.047). Paired t -tests for the L/M-cone opponent stimuli showed a significant loss of BOLD response at the high (8 Hz) temporal frequency compared to the low (2 Hz; $t(4) = 3.9, p = 0.018$). For the S-cone opponent stimuli, there was a significant loss of BOLD response at the high (8 Hz) temporal frequency compared to both the low (2 Hz; $t(4) = 4.6, p = 0.01$) and the mid- (4 Hz; $t(4) = 3.1, p = 0.038$) temporal frequencies.

The chromatic response across temporal frequency differs significantly between areas V4 and MT (Figures 5 and 9, see legend of Figure 9 for the ANOVA details). For area MT, response across temporal frequency is relatively flat and we found no significant effect of temporal

frequency on BOLD responses for either chromatic stimulus in comparison to the low-pass effects characteristic of V4.

Discussion

BOLD response to temporal frequency in the human LGN

The human LGN displays a significant loss of response at the highest temporal frequency tested (16 Hz) compared

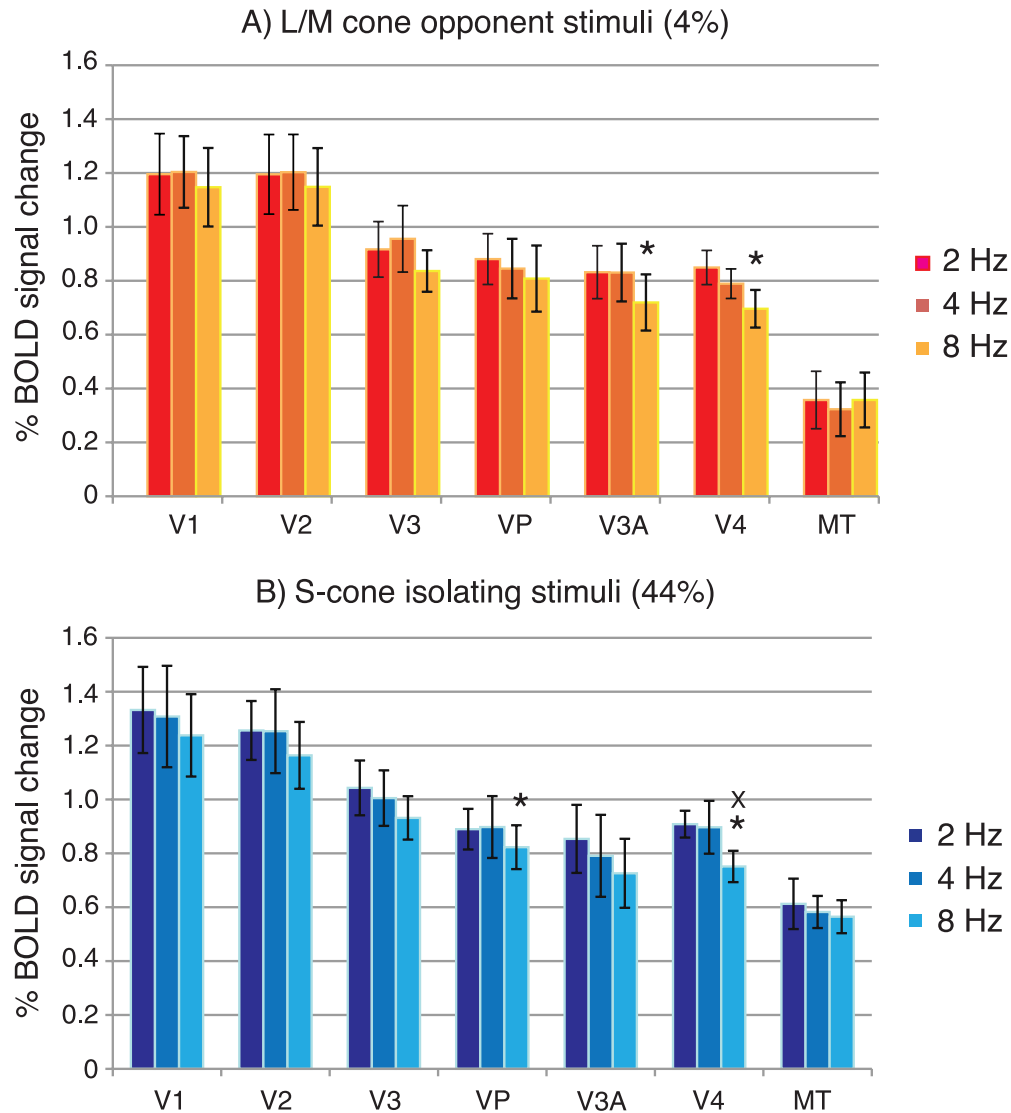


Figure 5. Results for chromatic stimuli in cortical areas V1, V2, V3, VP, V3A, V4, and MT. Percent BOLD signal is plotted as a function of 3 temporal frequencies (TF; 2, 4, and 8 Hz) in each cortical area for chromatic stimuli that isolate (A) the L/M-cone opponent response and (B) the S-cone isolating response. The means ± 1 SE for five subjects (all conditions) are shown. Data were analyzed using ANOVAs (see Statistical analyses and Results sections). For L/M-cone opponent responses, no effect of temporal frequency was evident in any area, with the exception of V4, which shows a reliable low-pass response to temporal frequency. For S-cone opponent responses, there was no effect of temporal frequency in V1, a trend for a low-pass response to temporal frequency in extrastriate areas (V2, V3, VP, V3A), and a reliable low-pass response for temporal frequency in V4; “*” indicates a significant ($p \leq 0.05$) difference from 2 Hz; “×” indicates a significant difference from 4 Hz.

to the two lower frequencies (2 and 8 Hz) at both high and low achromatic contrasts. The low-pass effect was most pronounced for the low-contrast stimuli, which showed a monotonic loss of signal with increasing temporal frequency, whereas for the high-contrast stimuli the response decline occurred only between 8 and 16 Hz. This low-pass dependence on temporal frequency is curious for two reasons. First, it is known that both M and P cells in the primate LGN, as assessed with single unit recordings, have an increasing response with temporal frequency from 2 to 16 Hz, displaying high-pass characteristics over this temporal range. Both cell types show responses that peak

in the range of 10–20 Hz with responses extending to higher temporal frequencies than can be detected behaviorally (Derrington & Lennie, 1984; Levitt et al., 2001). Thus, our results reveal a marked discrepancy between how single cell and BOLD responses depend on temporal frequency in the LGN. Second, it is curious that the most pronounced low-pass effect was found at low contrasts. Low contrasts favor the M cell over the P cell response (Kaplan & Shapley, 1982; Sclar et al., 1990) and would have been expected to reveal a high-pass dependence on temporal frequency, as found in the M cell group over this temporal range (Derrington & Lennie, 1984; Levitt et al.,

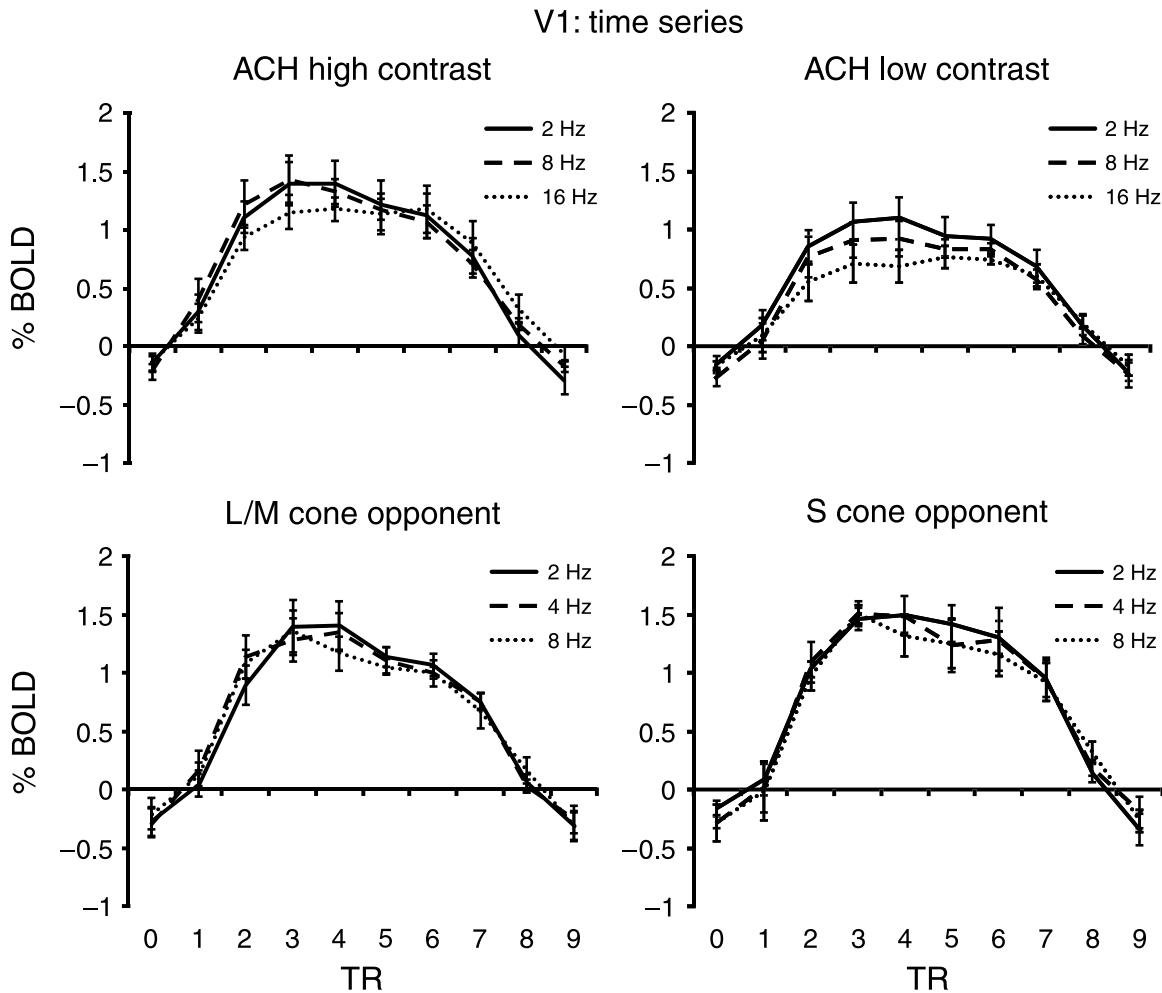


Figure 6. Time series data for V1 showing each temporal frequency (solid, dashed, and dotted lines) and each color condition (Ach high contrast, Ach low contrast, L/M-cone opponent, and S-cone opponent) as marked. Details as for Figure 3.

2001). Hence, our results suggest that the BOLD response of the LGN does not reflect the contribution of the M cell population. The low-pass BOLD responses of the LGN for achromatic stimuli contrast sharply with the high-pass responses of area MT, which shows the activity expected of a cortical area dominated by a response originating in the M cells of the LGN (Derrington & Lennie, 1984). This indicates that the M cell pathway at the LGN level is not well isolated in the BOLD response.

These two factors highlight the fact that the link between BOLD responses and those of single cells is a complex one. The fMRI BOLD response is weighted by many factors; the population size of each type of cell responding to the stimulus and their contrast gains are clearly important, but it is also thought that spiking activity may not be the main driver of BOLD activity as synaptic and local field potential activities are also known to weight the BOLD response (Logothetis, Pauls, Augath, Trinath, & Oeltermann, 2001). Analyses of thalamic processing identify at least two separate neural processes corresponding to neurons that are either “drivers” or “modulators”

(Reichova & Sherman, 2004; Sherman & Guillory, 1996, 1998, 2002). “Drivers” refers to neurons that transmit the information to be relayed from sensory end organs, whereas “modulators” serve to modulate the thalamic transmission of the driver input. Descending cortical pathways from V1, mostly originating from layer 6 (Van Horn & Sherman, 2004), have been shown to modulate the response properties of LGN cells in primates (Marrocco, McClurkin, & Alkire, 1996). We therefore speculate that that the reduced fMRI activation we find at high temporal frequencies reflects the modulatory control of the LGN because BOLD activations are produced by local field potentials as much, or more than, action potentials (Logothetis et al., 2001), and because only a minority of LGN synaptic junctions subserve driver-based activity (Sherman & Guillory, 1998). V1 neurons are known to have additional temporal filtering that reduces their response to high temporal frequencies (Foster et al., 1985) and so it seems likely that the LGN BOLD response reflects the descending cortical influences rather than the ascending driver pathways. We also note that our result

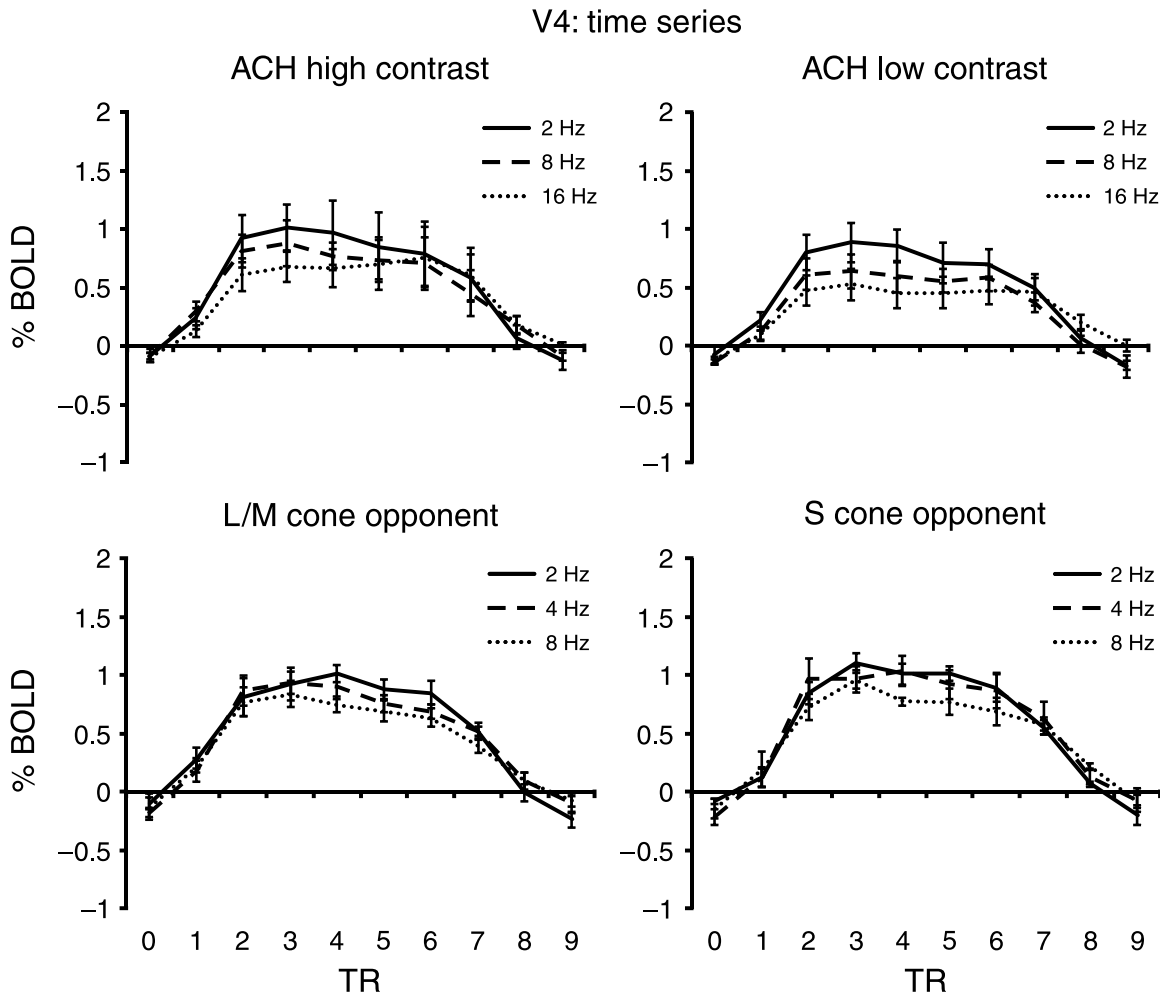


Figure 7. Time series data for V4 showing each temporal frequency (solid, dashed, and dotted lines) and each color condition (Ach high contrast, Ach low contrast, L/M-cone opponent, and S-cone opponent) as marked. Details as for Figure 3.

differs from that of Kastner et al. (2004), who reported that the BOLD response in the LGN had a high-pass shape, increasing with temporal frequency. Possible reasons why the two data sets differ are discussed further below.

There have been no studies of chromatic responses to temporal frequency in LGN. We find that the responses of both the L/M-cone opponent and S-cone opponent pathways are flat between 2 and 8 Hz. We did not measure chromatic responses at 16 Hz as stimuli were perceived to be very faint and achromatic; the faint appearance means that our attentional control would not work well, and the achromatic appearance suggest that chromatic mechanisms are not well isolated at this high temporal frequency. We measured a temporal contrast sensitivity function, using ring stimuli identical to those used in the scanning experiments and results based on the averaged data for two of the subjects are plotted in Figure 10. Data show the improvement in sensitivity produced at 16 Hz for the chromatic stimuli by the intrusion of this achromatic effect at threshold (dashed lines) compared to

a purely chromatic threshold (solid lines). We also note that the BOLD LGN responses, which show no significant dependence on temporal frequency, are discrepant from the psychophysical data (Figure 10), which show a low-pass chromatic effect with significant declines between 2 and 8 Hz, supporting the widely held conclusion that additional filtering at the cortical level limits the behavioral response.

BOLD response to temporal frequency in the human striate cortex

V1 shows a weak low-pass dependence on temporal frequency for achromatic contrasts and a stronger effect is found in other extrastriate areas (V2, V3, V3A, VP, and V4), with the exception of MT that shows an entirely different effect, to which we will return below. The low-pass nature of the V1 response is of interest because it is known that the synaptic input in layer 4C from the LGN has high temporal resolution (Viswanathan & Freeman,

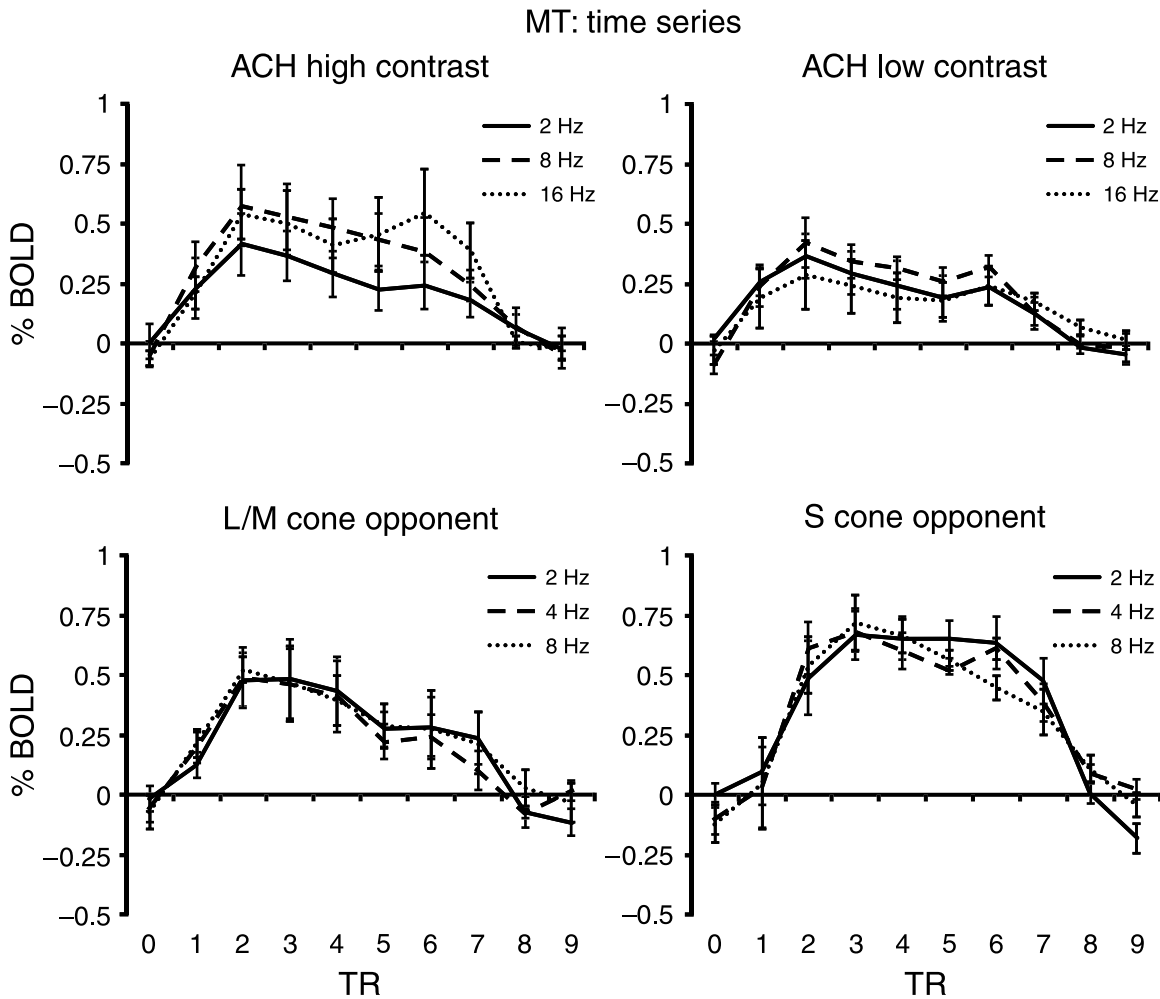
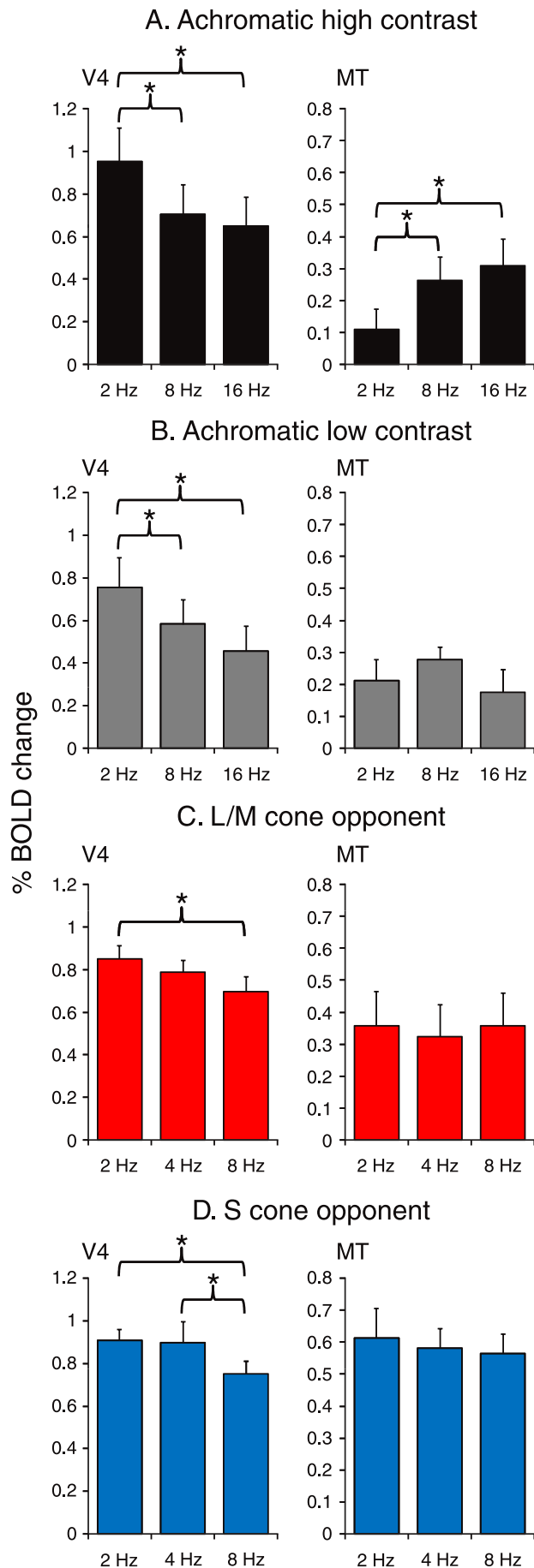


Figure 8. Time series data for MT showing each temporal frequency (solid, dashed, and dotted lines) and each color condition (Ach high contrast, Ach low contrast, L/M-cone opponent, and S-cone opponent) as marked. Details as for Figure 3.

2007) and it has been suggested that the BOLD signal is biased to synaptic activity (Logothetis et al., 2001; Viswanathan & Freeman, 2007). If this were so, one would have expected to see a stronger response to high temporal frequencies from V1 compared with other nearby cortical areas, which we do not find. Our results are consistent with a previous optical imaging study of the responses of V1 to sinusoidal temporal modulation in a prosimian primate (bush baby), which also showed a low-pass dependence on temporal frequency from 2 to 10 Hz (Khaytin et al., 2008).

Two previous fMRI studies have investigated the effect of temporal frequency for achromatic stimuli and these have produced differing results. Singh et al. (2000) used spatiotemporally sinusoidally modulated stimuli, as we used here. Like ours, their results show a loss of response between 9 and 18 Hz, although overall they had a more band-pass effect with a peak in response at 9 Hz compared to 2 Hz, which may be a result of the higher spatial frequency used (2 cycles/degree). Curiously, they also report a clear loss of response at higher temporal

frequencies for area MT, showing similar band-pass results as were found for the other cortical areas. It is not clear why their MT results differ from ours. Kastner et al. (2004), on the other hand, report a high-pass dependence for temporal frequency for all cortical areas, including MT, a pattern that clearly differs from our own results. Two factors may account for this difference. First, Kastner et al. (2004) defined temporal frequency as half a cycle (stimulus on or stimulus off) so effectively doubling the reported temporal frequency value compared to the full cycle frequency, and taking this into account, the three temporal frequencies actually measured were 0.25, 3.75, and 10 Hz. Hence, any loss of response at high temporal frequencies (above 10 Hz) may have been missed, although we still find clear low-pass effects even within the range used by Kastner et al. (2004). Second, Kastner et al. (2004) use spatiotemporally square-wave stimuli (checkerboard with abrupt onset and offset). The use of square waveforms spreads the spatiotemporal representation across frequency by introducing spatial and temporal higher harmonics, producing a broadband



temporal frequency stimulus, so confounding any interpretation of the shape of the temporal frequency dependence. An effective investigation of the effect of temporal frequency requires stimuli to be sinusoidally represented and so confined to a narrow band of spatiotemporal frequencies, as was used in our study and that of Singh et al. (2000). Additionally, it is known that the use of square-wave stimuli reveals dynamic non-linearities of temporal summation in the response of cortical neurons in cat area 17 (Dean, Tolhurst, & Walker, 1982; Tolhurst, Walker, Thompson, & Dean, 1980) and primate area V1 (Reid, Victor, & Shapley, 1992; Williams & Shapley, 2007), which boost the response to higher temporal frequencies (e.g. for transient onsets), although this explanation remains to be tested for BOLD responses. One other fMRI study (Mirzajani, Riyahi-Alam, Oghabian, Saberi, & Firouznia, 2007) that used square-wave checkerboards also reported a high-pass dependence on temporal frequency for large-sized checks (similar to Kastner et al., 2004) supporting the idea that the spatiotemporal spectrum of the stimulus is influential.

Individual cortical neurons in V1 show a low-pass dependence on temporal frequency or are very broadly tuned and typically show significant loss of response to high temporal frequencies (above 10 Hz; Foster et al., 1985). Thus, our results demonstrate a broadly similar low-pass dependence on temporal frequency as is found in single neurons of primate V1.

The BOLD responses for V1 found here, however, do not match the psychophysical response to the same stimuli very well. The contrast sensitivity function for our achromatic stimuli (Figure 10) shows a moderate peak at 8 Hz with a decline at both lower and high temporal frequencies, resembling previously published results for grating stimuli of 0.5 cycle/degree (Robson, 1966). The

Figure 9. A comparison of BOLD results for cortical areas (left) V4 and (right) MT for: (A) achromatic high contrast, (B) achromatic low contrast, (C) chromatic L/M-cone opponent, and (D) chromatic S-cone opponent stimuli. Percent BOLD signal is plotted as a function of 3 temporal frequencies (2, 8, and 16 Hz for achromatic stimuli and 2, 4, and 8 Hz for chromatic stimuli). Data are replotted from Figures 4 and 5. For V4, high- and low-contrast achromatic, L/M-cone opponent, and S-cone opponent conditions all show a reliable low-pass response to temporal frequency. For MT, the high-contrast achromatic condition shows a reliable high-pass response to temporal frequency. Low-contrast achromatic, L/M-cone opponent, and S-cone opponent conditions, however, are all flat across temporal frequency; “**” indicates a significant difference between conditions as marked ($p \leq 0.05$). Post-hoc ANOVAs compared differences in temporal frequency responses across area or contrast. These show that areas V4 and MT have a significantly different pattern of responses for all conditions (Ach high contrast $F(1, 2) = 35.8, p = 0.003$; Ach low contrast $F(1, 2) = 7.8, p = 0.02$; L/M-cone opponent $F(1, 2) = 22.3, p = 0.004$; S-cone opponent $F(1, 2) = 12.7, p = 0.003$). They also show that the pattern of responses in MT is significantly different between the Ach high- and low-contrast conditions ($F(1, 2) = 13.2, p = 0.006$).

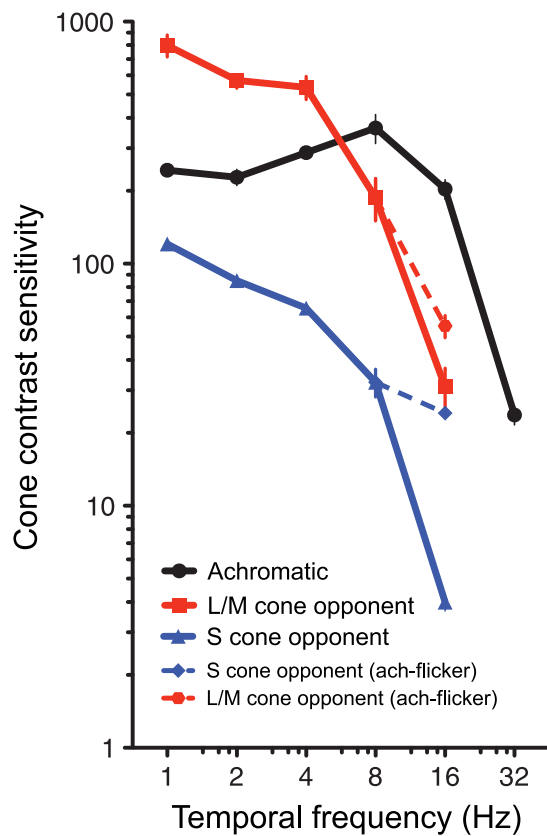


Figure 10. Temporal cone contrast sensitivity functions measured psychophysically on 2 of our 6 subjects (KTM and RFH) for the same stimuli as used in the fMRI experiments (black lines: achromatic stimuli, red lines: L/M-cone opponent stimuli, blue lines: S-cone opponent stimuli). Data points and solid lines show means and SE of data combined across subjects. Data points and dashed lines show the detection thresholds obtained at 16 Hz for L/M-cone opponent and S-cone opponent stimuli, which were achromatic in appearance at this temporal frequency, whereas data points with solid lines show thresholds for detection of color at 16 Hz. (For all other temporal frequencies, chromatic stimuli all appeared colored at detection threshold.)

BOLD cortical results for V1, on the other hand, are clearly more low pass than the psychophysical results. A poor association between the psychophysical threshold and cortical (V1 and V2) BOLD response has been demonstrated previously (Mullen et al., 2007) and is not surprising in view of the differences in origins of the two signals, the stimulus contrasts involved, and the differences in the size and selectivity of the neural populations supporting high-contrast BOLD signals as opposed to low-contrast detection thresholds (Schluppeck & Engel, 2002).

Our results are the first systematic comparison of the effect of temporal frequency on chromatic BOLD responses using narrowband sinusoidal modulations. We find that both L/M- and S-cone opponent chromatic responses are relatively flat in V1 in the temporal range

measured (2–8 Hz) with no significant effects of temporal frequency, and the BOLD response in this area is relatively more maintained than the psychophysical contrast sensitivity function (Figure 10), which declines significantly after 4 Hz suggesting further temporal filtering occurs at a subsequent stage. One study has reported that BOLD signals can be recorded in V1 for temporal frequency flicker that cannot be resolved psychophysically (Jiang et al., 2007).

BOLD response to temporal frequency in the human extrastriate cortex

Results for the achromatic stimuli for extrastriate areas V2, V3, VP, and V3A display the same low-pass dependence on temporal frequency as was found for V1 at both high and low contrasts. Neurons have a similar low-pass temporal dependence in V2 as is found for V1 (Foster et al., 1985; Levitt, Yoshioka, & Lund, 1994) and so the continuation of this trend to V2 is not surprising. The results for V3A are more surprising, however, as human V3A is believed to be the homologue of area V3 in the primate, and the latter is thought to form part of the dorsal pathway leading to MT, based on the sensitivity of its neurons to higher temporal frequencies than in V2, a high-contrast sensitivity, and strong direction selectivity (Gegenfurtner, Kiper, & Levitt, 1997). Previous fMRI results have shown a high sensitivity to motion and relatively reduced BOLD response to chromatic compared to achromatic stimuli in V3A, supporting its association with the dorsal pathway (Liu & Wandell, 2005; Mullen et al., 2007; Tootell et al., 1997). Here we find similar temporal properties for V2, V3, VP, and V3A but very different temporal properties for MT, contrary to what would be expected if V3A forms part of the dorsal pathway. This result may reflect the fact that V3A is not exclusively dorsal since the equivalent primate area (V3) receives inputs from both M and P cell pathways and projects to both MT and V4 (Gegenfurtner et al., 1997). Hence, a response pattern to temporal frequency characteristic of the dorsal pathway may not be revealed under our stimulus conditions.

A comparison of areas MT and V4

The high-pass responses of area MT for achromatic stimuli contrast sharply with the low-pass responses of the other cortical areas and the LGN. At high contrasts, area MT shows a highly significant monotonically rising response with temporal frequency. This effect is less apparent at low contrast, although response is maintained with increasing temporal frequency. The low-contrast data may be less reliable due to the lower subject numbers (4 instead of 5), a smaller signal at lower contrasts, or it

may reveal a genuine difference of contrast gain between temporal frequencies as noted in the results. The LGN M cells are thought to provide the dominant input to area MT (Maunsell et al., 1990; Tootell et al., 1995). Our high-pass results resemble the typical LGN M cell responses to temporal frequency (Derrington & Lennie, 1984) and so lend support to this association, although we note that LGN M and P cell responses to temporal frequency are very similar (Derrington & Lennie, 1984; Levitt et al., 2001). It is interesting that the low-pass cortical filtering found in the early cortical areas V1, V2, and even the LGN itself is not reflected in the BOLD response of area MT, indicating that this projection may require more specialized stimuli to be revealed at earlier stages in the visual pathway. Our BOLD responses may be enhanced by the very high-contrast sensitivity of area MT, which is higher than the LGN due to spatial summation effects (Sclar et al., 1990; Tootell et al., 1995). Our results differ from Singh et al. (2000), who found a band-pass dependence on temporal frequency with significant decline between 9 and 18 Hz. It is not clear why their results differ from ours, except that our low spatial frequency stimuli (0.5 cycle/degree) are better suited to activation of MT than their mid-range one (2 cycles/degree). Kastner et al. (2004) did not record above 10 Hz (although their data were labeled as 20 Hz).

We were able to obtain robust chromatic BOLD responses from MT despite the overall lower responsiveness of MT for chromatic compared to achromatic stimuli (Liu & Wandell, 2005; Mullen et al., 2007; Wandell et al., 1999), and this is probably due to the high chromatic contrasts used corresponding 25 and 37 times average threshold for RG and BY stimuli, respectively. Our results show that the BOLD chromatic response is maintained across temporal frequency between 2 and 8 Hz. The level of response of MT neurons to chromatic modulation is controversial, but there is at least some response (Gegenfurtner et al., 1994; Seidemann, Poirson, Wandell, & Newsome, 1999). The chromatic activation of MT is likely to be based on the response of LGN M cells to chromatic modulation (Derrington, Krauskopf, & Lennie, 1984), originating in the retina (Lee et al., 1990), which is thought to contribute psychophysically to chromatic motion thresholds (Mullen, Yoshizawa, & Baker, 2003). We note, however, that direct projections to MT of koniocellular cells from the LGN (Sincich, Park, Wohlgemuth, & Horton, 2004) and P cells via V1 (Nassi, Lyon, & Callaway, 2006) may also contribute.

Our results show very significant differences in the processing of temporal frequency in MT compared to V4, highlighted in Figure 9. V4 has significant low-pass dependence on temporal frequency for all stimuli, both high and low achromatic contrasts, and both chromatic contrasts, in contrast to the high-pass or flat responses in MT. These effects are supported by results of previous studies, although only two temporal frequencies were used and comparisons across temporal frequency were not

made within scans (Liu & Wandell, 2005; Wade et al., 2008). Overall, our results show that the human ventral pathway becomes progressively more low-pass from V1 to V4, with V4 having a limited temporal processing capacity for both chromatic and achromatic stimulations. This pathway ultimately supports a slow processing of object recognition in high-level object-selective regions such as FFA or PPA (McKeeff, Remus, & Tong, 2007). The dorsal pathway, on the other hand, becomes more high pass at MT, ultimately supporting its role in motion processing and guiding motor actions. We conclude that the dorsal and ventral pathways of human vision progressively develop significant and characteristic differences in temporal processing that affect both chromatic and achromatic stimuli.

Acknowledgments

This work was supported by the following grants: a Wesley Institute Research Grant (Brisbane, Australia), CIHR Grants (#MOP-10819) to KTM and (# MOP53346) to RFH, and an NSERC Grant (RGPIN 183625-05) to KTM. We thank Dr. Katie McMahon for her expert help in the scanning room and we would like to thank all of our subjects for giving up their time.

Commercial relationships: none.

Corresponding author: Kathy T. Mullen.

Email: kathy.mullen@mcgill.ca.

Address: McGill Vision Research (H4.14), Department of Ophthalmology, 687 Pine Ave West, Montreal, QC H3A 1A1, Canada.

Footnote

¹We use the color terms “red–green” (RG) and “blue–yellow” (BY) to refer to the stimuli that activate L/M-cone opponent and S/(L + M)-cone opponent mechanisms, respectively. These cone opponent processes when activated selectively by the cardinal stimuli do not give rise to the unique color sensations of red, green, blue, or yellow and so should not be confused with *color* opponent processes.

References

- Benjamini, Y., & Hochberg, Y. (1995). Controlling the false discovery rate—A practical and powerful approach to multiple testing. *Journal of the Royal Statistical Society B: Methodological*, 57, 289–300.

- Bradley, A., Zang, L., & Thibos, L. N. (1992). Failures of isoluminance caused by ocular chromatic aberration. *Applied Optics, 31*, 3657–3667.
- Brainard, D. H. (1997). The psychophysics toolbox. *Spatial Vision, 10*, 433–436.
- Brefczynski, J. A., & DeYoe, E. A. (1999). A physiological correlate of the “spotlight” of visual attention. *Nature Neuroscience, 2*, 370–374.
- Brewer, A. A., Liu, J., Wade, A. R., & Wandell, B. A. (2005). Visual field maps and stimulus selectivity in human ventral occipital cortex. *Nature Neuroscience, 8*, 1102–1109.
- Cole, G. R., & Hine, T. (1992). Computation of cone contrasts for color vision research. *Behavioural Research, Methods and Instrumentation, 24*, 22–27.
- Cole, G. R., Hine, T., & McIlhagga, W. (1993). Detection mechanisms in L-, M-, and S-cone contrast space. *Journal of the Optical Society of America A, 10*, 38–51.
- Cottaris, N. P. (2003). Artifacts in spatiochromatic stimuli due to variations in preretinal absorption and axial chromatic aberration: Implications for color physiology. *Journal of the Optical Society of America A, Optics, Image Science, and Vision, 20*, 1694–1713.
- Dean, A. F., Tolhurst, D. J., & Walker, N. S. (1982). Non-linear temporal summation by simple cells in cat striate cortex demonstrated by failure of superposition. *Experimental Brain Research, 45*, 456–458.
- Derrington, A. M., Krauskopf, J., & Lennie, P. (1984). Chromatic mechanisms in lateral geniculate nucleus of macaque. *The Journal of Physiology, 357*, 241–265.
- Derrington, A. M., & Lennie, P. (1984). Spatial and temporal contrast sensitivities of neurones in lateral geniculate nucleus of macaque. *The Journal of Physiology, 357*, 219–240.
- Dumoulin, S. O., Hoge, R. D., Baker, C. L., Jr., Hess, R. F., Achtman, R. L., & Evans, A. C. (2003). Automatic volumetric segmentation of human visual retinotopic cortex. *Neuroimage, 18*, 576–587.
- Engel, S., Zhang, X., & Wandell, B. (1997). Colour tuning in human visual cortex measured with functional magnetic resonance imaging. *Nature, 388*, 68–71.
- Engel, S. A., Rumelhart, D. E., Wandell, B. A., Lee, A. T., Glover, G. H., Chichilnisky, E. J., et al. (1994). fMRI of human visual cortex. *Nature, 369*, 525.
- Foster, K. H., Gaska, J. P., Nagler, M., & Pollen, D. A. (1985). Spatial and temporal frequency selectivity of neurones in visual cortical areas V1 and V2 of the macaque monkey. *The Journal of Physiology, 365*, 331–363.
- Gandhi, S. P., Heeger, D. J., & Boynton, G. M. (1999). Spatial attention affects brain activity in human primary visual cortex. *Proceedings of the National Academy of Sciences of the United States of America, 96*, 3314–3319.
- Gegenfurtner, K. R., Kiper, D. C., Beusmans, J. M., Carandini, M., Zaidi, Q., & Movshon, J. A. (1994). Chromatic properties of neurons in macaque MT. *Visual Neuroscience, 11*, 455–466.
- Gegenfurtner, K. R., Kiper, D. C., & Levitt, J. B. (1997). Functional properties of neurons in macaque area V3. *Journal of Neurophysiology, 77*, 1906–1923.
- Hadjikhani, N., Liu, A. K., Dale, A. M., Cavanagh, P., & Tootell, R. B. (1998). Retinotopy and color sensitivity in human visual cortical area V8. *Nature Neuroscience, 1*, 235–241.
- Hess, R. F., Thompson, B., Gole, G., & Mullen, K. T. (2009). Deficient responses from the lateral geniculate nucleus in humans with amblyopia. *European Journal of Neuroscience, 29*, 1064–1070.
- Jiang, Y., Zhou, K., & He, S. (2007). Human visual cortex responds to invisible chromatic flicker. *Nature Neuroscience, 10*, 657–662.
- Kaplan, E., & Shapley, R. M. (1982). X and Y cells in the lateral geniculate nucleus of macaque monkeys. *The Journal of Physiology, 330*, 125–143.
- Kastner, S., O'Connor, D. H., Fukui, M. M., Fehd, H. M., Herwig, U., & Pinsk, M. A. (2004). Functional imaging of the human lateral geniculate nucleus and pulvinar. *Journal of Neurophysiology, 91*, 438–448.
- Kelly, D. H. (1983). Spatiotemporal variation of chromatic and achromatic contrast thresholds. *Journal of the Optical Society of America, 73*, 742–750.
- Khaytin, I., Chen, X., Royal, D. W., Ruiz, O., Jermakowicz, W. J., Siegel, R. M., et al. (2008). Functional organization of temporal frequency selectivity in primate visual cortex. *Cerebral Cortex, 18*, 1828–1842.
- Kleinschmidt, A., Lee, B. B., Requardt, M., & Frahm, J. (1996). Functional mapping of color processing by magnetic resonance imaging of responses to selective P- and M-pathway stimulation. *Experimental Brain Research, 110*, 279–288.
- Lankheet, M. J., Lennie, P., & Krauskopf, J. (1998). Temporal-chromatic interactions in LGN P-cells. *Visual Neuroscience, 15*, 47–54.
- Lee, B. B., Pokorny, J., Smith, V. C., Martin, P. R., & Valberg, A. (1990). Luminance and chromatic modulation sensitivity of macaque ganglion cells and human observers. *Journal of the Optical Society of America A, 7*, 2223–2236.

- Levitt, J. B., Schumer, R. A., Sherman, S. M., Spear, P. D., & Movshon, J. A. (2001). Visual response properties of neurons in the LGN of normally reared and visually deprived macaque monkeys. *Journal of Neurophysiology*, 85, 2111–2129.
- Levitt, J. B., Yoshioka, T., & Lund, J. S. (1994). Intrinsic cortical connections in macaque visual area V2: Evidence for interaction between different functional streams. *Journal of Comparative Neurology*, 342, 551–570.
- Liu, J., & Wandell, B. A. (2005). Specializations for chromatic and temporal signals in human visual cortex. *Journal of Neuroscience*, 25, 3459–3468.
- Logothetis, N. K., Pauls, J., Augath, M., Trinath, T., & Oeltermann, A. (2001). Neurophysiological investigation of the basis of the fMRI signal. *Nature*, 412, 150–157.
- Marrocco, R. T., McClurkin, J. W., & Alkire, M. T. (1996). The influence of the visual cortex on the spatiotemporal response properties of lateral geniculate nucleus cells. *Brain Research*, 737, 110–118.
- Maunsell, J. H., Nealey, T. A., & DePriest, D. D. (1990). Magnocellular and parvocellular contributions to responses in the middle temporal visual area (MT) of the macaque monkey. *Journal of Neuroscience*, 10, 3323–3334.
- McKeeff, T. J., Remus, D. A., & Tong, F. (2007). Temporal limitations in object processing across the human ventral visual pathway. *Journal of Neurophysiology*, 98, 382–393.
- McKeefry, D. J., & Zeki, S. (1997). The position and topography of the human colour centre as revealed by functional magnetic resonance imaging. *Brain*, 120, 2229–2242.
- Mirzajani, A., Riyahi-Alam, N., Oghabian, M. A., Saberi, H., & Firouznia, K. (2007). Spatial frequency modulates visual cortical response to temporal frequency variation of visual stimuli: An fMRI study. *Physiological Measurement*, 28, 547–554.
- Mullen, K. T. (1985). The contrast sensitivity of human colour vision to red–green and blue–yellow chromatic gratings. *The Journal of Physiology*, 359, 381–400.
- Mullen, K. T., Dumoulin, S. O., & Hess, R. F. (2008). Color responses of the human lateral geniculate nucleus: Selective amplification of S-cone signals between the lateral geniculate nucleus and primary visual cortex measured with high-field fMRI. *European Journal of Neuroscience*, 28, 1911–1923.
- Mullen, K. T., Dumoulin, S. O., McMahon, K. L., De Zubiray, G. I., & Hess, R. F. (2007). Selectivity of human retinotopic visual cortex to S-cone-opponent, L/M-cone-opponent and achromatic stimulation. *European Journal of Neuroscience*, 25, 491–502.
- Mullen, K. T., Thompson, B., & Hess, R. F. (2008). Responses of the human LGN to different temporal frequencies for achromatic, L/M cone opponent and S-cone opponent stimuli measured with high field fMRI [Abstract]. *Journal of Vision*, 8(6):808, 808a, <http://www.journalofvision.org/content/8/6/808>, doi:10.1167/8.6.808.
- Mullen, K. T., Yoshizawa, T., & Baker, C. L. (2003). Luminance mechanisms mediate the motion of red–green isoluminant gratings: The role of “temporal chromatic aberration”. *Vision Research*, 43, 1235–1247.
- Nassi, J. J., Lyon, D. C., & Callaway, E. M. (2006). The parvocellular LGN provides a robust disynaptic input to the visual motion area MT. *Neuron*, 50, 319–327.
- O’Connor, D. H., Fukui, M. M., Pinsk, M. A., & Kastner, S. (2002). Attention modulates responses in the human lateral geniculate nucleus. *Nature Neuroscience*, 5, 1203–1209.
- Ogawa, S., Lee, T. M., Kay, A. R., & Tank, D. W. (1990). Brain magnetic resonance imaging with contrast dependent on blood oxygenation. *Proceedings of the National Academy of Sciences of the United States of America*, 87, 9868–9872.
- Pelli, D. G. (1997). The Videotoolbox software for visual psychophysics: Transforming numbers into movies. *Spatial Vision*, 10, 437–442.
- Reichova, I., & Sherman, S. M. (2004). Somatosensory corticothalamic projections: Distinguishing drivers from modulators. *Journal of Neurophysiology*, 92, 2185–2197.
- Reid, R. C., & Shapley, R. M. (2002). Space and time maps of cone photoreceptor signals in macaque lateral geniculate nucleus. *Journal of Neuroscience*, 22, 6158–6175.
- Reid, R. C., Victor, J. D., & Shapley, R. M. (1992). Broadband temporal stimuli decrease the integration time of neurons in cat striate cortex. *Visual Neuroscience*, 9, 39–45.
- Robson, J. G. (1966). Spatial and temporal contrast-sensitivity functions of the visual system. *Journal of the Optical Society of America*, 56, 1141–1142.
- Sankeralli, M. J., & Mullen, K. T. (1996). Estimation of the L-, M-, and S-cone weights of the postreceptorial detection mechanisms. *Journal of the Optical Society of America A*, 13, 906–915.
- Sankeralli, M. J., & Mullen, K. T. (1997). Postreceptorial chromatic detection mechanisms revealed by noise masking in three-dimensional cone contrast space. *Journal of the Optical Society of America A*, 14, 2633–2646.
- Schluppeck, D., & Engel, S. A. (2002). Color opponent neurons in V1: A review and model reconciling results from imaging and single-unit recording.

- Journal of Vision*, 2(6):5, 480–492, <http://www.journalofvision.org/content/2/6/5>, doi:10.1167/2.6.5. [PubMed] [Article]
- Schneider, K. A., Richter, M. C., & Kastner, S. (2004). Retinotopic organization and functional subdivisions of the human lateral geniculate nucleus: A high-resolution functional magnetic resonance imaging study. *Journal of Neuroscience*, 24, 8975–8985.
- Sclar, G., Maunsell, J. H., & Lennie, P. (1990). Coding of image contrast in central visual pathways of the macaque monkey. *Vision Research*, 30, 1–10.
- Seidemann, E., Poirson, A. B., Wandell, B. A., & Newsome, W. T. (1999). Color signals in area MT of the macaque monkey. *Neuron*, 24, 911–917.
- Shapley, R. (1982). Parallel pathways in the mammalian visual system. *Annals of the New York Academy of Sciences*, 388, 11–20.
- Sherman, S. M., & Guillery, R. W. (1996). Functional organization of thalamocortical relays. *Journal of Neurophysiology*, 76, 1367–1395.
- Sherman, S. M., & Guillery, R. W. (1998). On the actions that one nerve cell can have on another: Distinguishing “drivers” from “modulators”. *Proceedings of the National Academy of Sciences of the United States of America*, 95, 7121–7126.
- Sherman, S. M., & Guillery, R. W. (2002). The role of the thalamus in the flow of information to the cortex. *Philosophical Transactions of the Royal Society of London B: Biological Sciences*, 357, 1695–1708.
- Sincich, L. C., Park, K. F., Wohlgemuth, M. J., & Horton, J. C. (2004). Bypassing V1: A direct geniculate input to area MT. *Nature Neuroscience*, 7, 1123–1128.
- Singh, K. D., Smith, A. T., and Greenlee, M. W. (2000). Spatiotemporal frequency and direction sensitivities of human visual areas measured using fMRI. *Neuroimage*, 12, 550–564.
- Smith, V. C., & Pokorny, J. (1975). Spectral sensitivity of the foveal cone photopigments between 400 and 500 nm. *Vision Research*, 15, 161–171.
- Somers, D. C., Dale, A. M., Seiffert, A. E., & Tootell, R. B. (1999). Functional MRI reveals spatially specific attentional modulation in human primary visual cortex. *Proceedings of the National Academy of Sciences of the United States of America*, 96, 1663–1668.
- Talairach, J., & Tournoux, P. (1988). *Co-planar stereotaxic atlas of the human brain*. New York: Thieme Medical.
- Tolhurst, D. J., Walker, N. S., Thompson, I. D., & Dean, A. F. (1980). Non-linearities of temporal summation in neurones in area 17 of the cat. *Experimental Brain Research*, 38, 431–435.
- Tootell, R. B., Mendola, J. D., Hadjikhani, N. K., Ledden, P. J., Liu, A. K., Reppas, J. B., et al. (1997). Functional analysis of V3A and related areas in human visual cortex. *Journal of Neuroscience*, 17, 7060–7078.
- Tootell, R. B., Reppas, J. B., Kwong, K. K., Malach, R., Born, R. T., Brady, T. J., et al. (1995). Functional analysis of human MT and related visual cortical areas using magnetic resonance imaging. *Journal of Neuroscience*, 15, 3215–3230.
- Van Horn, S. C., & Sherman, S. M. (2004). Differences in projection patterns between large and small corticothalamic terminals. *Journal of Computer Neurology*, 475, 406–415.
- Vaughan, J. T., Adriany, G., Garwood, M., Yacoub, E., Duong, T., Delabarre, L., et al. (2002). Detunable transverse electromagnetic (TEM) volume coil for high-field NMR. *Magnetic Resonance in Medicine*, 47, 990–1000.
- Viswanathan, A., & Freeman, R. D. (2007). Neuro-metabolic coupling in cerebral cortex reflects synaptic more than spiking activity. *Nature Neuroscience*, 10, 1308–1312.
- Wade, A., Augath, M., Logothetis, N., & Wandell, B. (2008). fMRI measurements of color in macaque and human. *Journal of Vision*, 8(10):6, 1–19, <http://www.journalofvision.org/content/8/10/6>, doi:10.1167/8.10.6. [PubMed] [Article]
- Wade, A. R. (2002). The negative BOLD signal unmasked. *Neuron*, 36, 993–995.
- Wade, A. R., Brewer, A. A., Rieger, J. W., & Wandell, B. A. (2002). Functional measurements of human ventral occipital cortex: Retinotopy and colour. *Philosophical Transactions of the Royal Society of London B: Biological Sciences*, 357, 963–973.
- Wandell, B. A., Brewer, A. A., & Dougherty, R. F. (2005). Visual field map clusters in human cortex. *Philosophical Transactions of the Royal Society of London B: Biological Sciences*, 360, 693–707.
- Wandell, B. A., Poirson, A. B., Newsome, W. T., Baseler, H. A., Boynton, G. M., Huk, A., et al. (1999). Color signals in human motion-selective cortex. *Neuron*, 24, 901–909.
- Williams, P. E., & Shapley, R. M. (2007). A dynamic nonlinearity and spatial phase specificity in macaque V1 neurons. *Journal of Neuroscience*, 27, 5706–5718.
- Zhang, Y., Teunissen, K., Song, W., & Li, X. (2008). Dynamic modulation transfer function: A method to characterize the temporal performance of liquid-crystal displays. *Optics Letters*, 33, 533–535.